ANALYSIS AND INTERCOMPARISON OF VARIOUS GLOBAL EVAPORATION PRODUCTS

Tsuyoshi Watabe and Masahisa Kubota[1]

School of Marine Science and Technology, Tokai University
3-20-1, Orido, Shimizu, Shizuoka, Shizuoka, JAPAN 424-8610
e-mail; tsuyoshi@mercury.oi.u-tokai.ac.jp

ABSTRACT

We analyzed evaporation data in the Japanese Ocean Flux Data Sets with Use of Remote Sensing Observations (J-OFURO) Ver.2. There exists huge evaporation in Gulf Stream, Kuroshio Extension, the ocean dessert and the southern part of the Indian Ocean. The temporal variation of evaporation is overwhelmingly large, of which the standard deviation is more than 120(mm), in the Kuroshio Extension region. Also, the result of harmonic analysis gives that this large variation is closely related to annual variation. In addition, the first EOF mode shows long-term variation showing the maximum amplitude between 1992 and 1994 and remarkable decrease after 1994, and large amplitude in the equatorial region and northeast of Australia. The second and third modes were strongly influenced by El Nino.

Moreover, we compared J-OFURO2 evaporation product with other products. We used six kinds of data sets (HOAPS3 and GSSTF2 of satellite data, NRA1, NRA2, ERA40 and JRA25 of reanalysis data) for comparison. Most products show underestimation in the most regions, in particular, in the northern North Pacific, mid-latitudes of the eastern South Pacific, and high-latitudes of the South Pacific compared with J-OFURO2. On the other hand, JRA25 and NRA2 show large overestimation in the equatorial regions. RMS difference between NRA2 and J-OFURO2 in the Kuroshio Extension was significantly large, more than 120(mm).

KEY WORDS: J-OFUROß2, EVAPORATION, SATELLITE DATA, REANALYSIS DATA

1. INTRODUCTION

Water resource has become to be a big issue for us because water is critical for us to survive. IT is said that the recent water distribution is inhomogeneous in the world as compared before. Evaporation and precipitation at the sea surface is the largest components compared with other many components in the water cycle. While many studies are related to precipitation, there are very few studies related to evaporation. However, evaporation should be important as well as precipitation in order to understand global water cycle. In the present study, we construct and analyze global evaporation data sets and carry out intercomparison of various data sets.

We introduce the data sets used in this study in section 2. Next, the global evaporation data derived from latent heat flux data in Japanese Ocean Flux data sets with Use of Remote sensing Observations (J-OFURO) (Kubota et al.,2002) are analyzed in section 3. The intercomparison results with other evaporation data are given in section 4. Finally some conclusions are given in section 5.

2. DATA

We used various global products shown in Table 1. Since the temporal and spatial resolutions are different depending on each product, all products are transformed into monthly data on 1° x 1° grid. The analysis period is from 1988 to 2000. We basically estimated evaporation using latent heat flux data, except for HOAPS and ERA40 those directly provide evaporation data.

3. ANALYSIS OF J-OFURO2 EVAPORATION DATA

Figure 1. shows the average evaporation field derived from J-OFURO2 latent heat flux. Basically there are high evaporation (more than 200 mm) regions called as ocean deserts in mid-latitudes. Also the evaporation is remarkably large over the western boundary current regions such as Kuroshio and Gulf Stream. Standard deviations are given in Fig. 2. The values are fairly small in most regions except western boundary current regions where the values are more than 80 mm. In particular it is interesting that the standard deviation over the Kuroshio is much larger than that over the Gulf Stream, though the average values over the Gulf Stream is larger than that over the Kuroshio. We carried out the Empirical Orthogonal Function(EOF) analysis. Figures 3.and 4 gives spatial patterns and time variation for the first three modes. The first mode suggests long-term variability of decrease from 1992 to 2001. The amplitudes are large in the eastern equatorial Pacific and east of Japan. The decrease east of Japan is consistent with Tomita and Kubota(2005). The second and the third modes appear to be related to El Nino/La Nina. It is interesting that the phase of the third mode is delayed compared with that of the second mode.

Also the third mode has a large amplitude east of Japan. Therefore, the third mode seems to represent influences by El Nino.

4. Intercomparison

. We compared J-OFURO2 evaporation product with other products, those are GSSTF2, HOAPS3, OA Flux, NRA1, NRA2, ERA40 and JRA25. Most products show underestimation in the northern North Pacific, mid-latitudes of the eastern South Pacific, and high-latitudes of the South Pacific. JRA25 and NRA2 show large overestimation in the equatorial regions, compared with J-OFURO2 evaporation (Fig.5). The RMS differences between NRA2 and J-OFURO2 are significantly large, more than 120 mm there (Fig.6). The large value is consistent with previous results by Kubota et al.(2008), in which they evaluate NRA2 latent heat flux using KEO buoy data.

5. CONCLUSION

We analyzed global evaporation data in J-OFURO2. High evaporation regions exist in mid-latitudes in both hemispheres and over the western boundary regions. The evaporation over the Gulf Stram is larger than that over the Kuroshio/Kuroshio Extension regions. On the other hand, the variability generally is small in most regions except over the western boundary current regions. It is interesting that the variability over the Kuroshio/Kuroshio Extension regions is much larger than that over the Gulf Stream region. The difference seems to be closely related to the more complicated flow pattern of the Kuroshio Extension than that of the Gulf Stream. Moreover, we carried out EOF analysis for the evaporation data. The first mode gives the long-term variability having the peak in 1992. Both of the second and third modes appear to be related to ENSO. The Second mode is directly related to ENSO itself, while the third mode is related to the influence of ENSO.

The J-OFURO2 evaporation field is compared with other global evaporation fields, i.e., GSSTF2, HOAPS3, OA Flux, NRA1, NRA2, ERA40 and JRA25. Most products show underestimation in the northern North Pacific, mid-latitudes of the eastern South Pacific, and high-latitudes of the South Pacific. JRA25 and NRA2 show large overestimation in the equatorial regions, compared with J-OFURO2 evaporation. The RMS differences between NRA2 and J-OFURO2 are significantly large, more than 120 mm there.

ACKNOWLEDGMENT:

This study was supported by the Japan Aerospace Exploration Agency.

REFERENCES:

Kubota, M., N. Iwasaka, S. Kizu, M. Konda and K. Kutsuwada, 2002: Japanese ocean flux data sets with use of remote sensing observations(J-OFURO), *J. Oceanogr.*, 58, 213-225.

Tomita, H. and M. Kubota, 2005: Increase in turbulent heat flux during the 1990's over the Kuroshio/Oyashio extension region, Geophys. Res. Lett., 32, L09795, DOI:10.1029/2004GL022075.

Table 1. Description of various evaporation products

Satellite data

Data Set	Japanese-Ocean Flux data sets with Use of Remote sensing Observations Version.2 (J-OFURO2)	Hamburg Ocean Atmosphere Parameters and Fluxes from Satellite Data 3 (HOAPS3)	Goddard Satellite-Based Surface Turbulent Fluxes 2 (GSSTF2)
Peiod	1988/1-2005/12	1987/7-2005/12	1987/7-2000/12
Spatial resolution	1°	1°	1°
Temporal resolution	Daily mean	12 hours mean	Daily mean

Re-analysis data

Data Set	NCEP/NCAR Re-analysis (NRA1)	NCEP-DOE Re-analysis (NRA2)	ECMWF Re-analysis 40 (ERA40)	Japanese Re-analysis 25 (JRA25)
Period	1948/1-present	1979/1-present	1957/9-2002/8	1979/7-present
Spatial resolution	Gaussian grid T62	Gaussian grid T62	Gaussian grid TL159	Gaussian grid T106
Temporal resolution	6 hours mean	6 hours mean	6 hours mean	6 hours mean

Hybrid data

Data Set	Objectively Analyzed Air-Sea Fluxes(OAFlux)
Period	1958/1-2006/12
Spatial resolution	1°
Temporal resolution	Daily mean

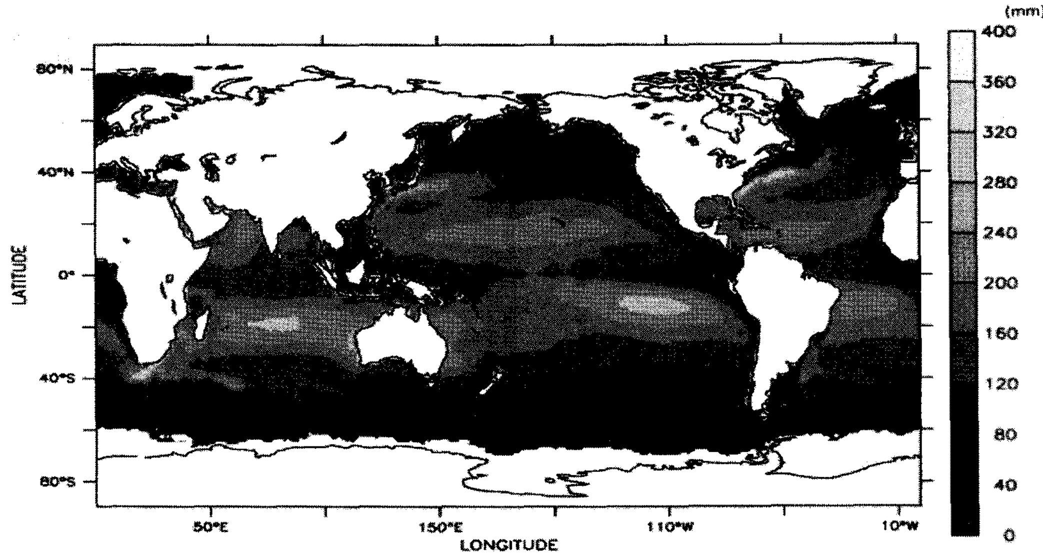

Figure 1. Average global evaporation field derived from J-OFURO2.

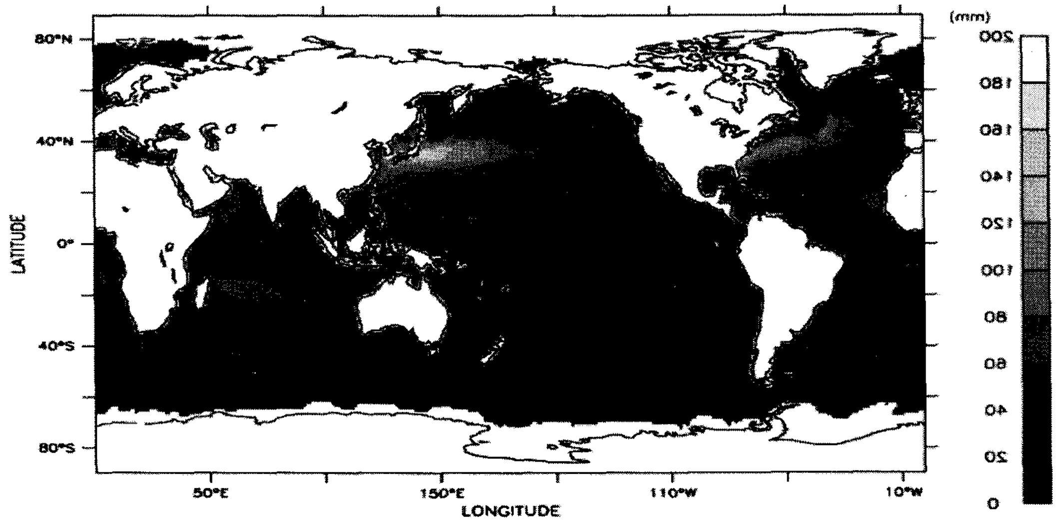

Figure 2. Standard deviation field of global evaporation derived from J-OFURO2.

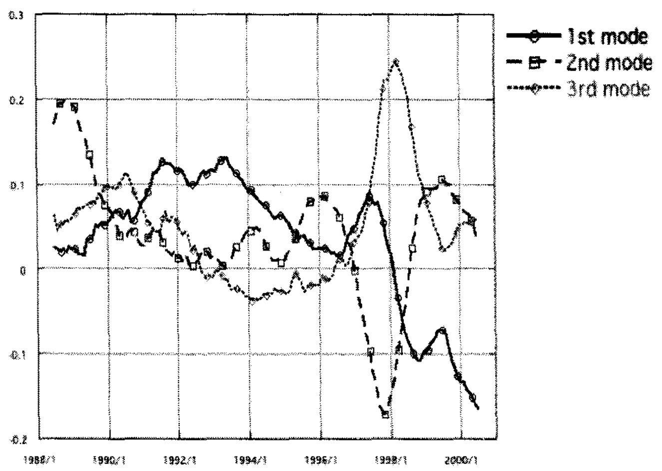

Figure 3. Time variation of eigenfunctions

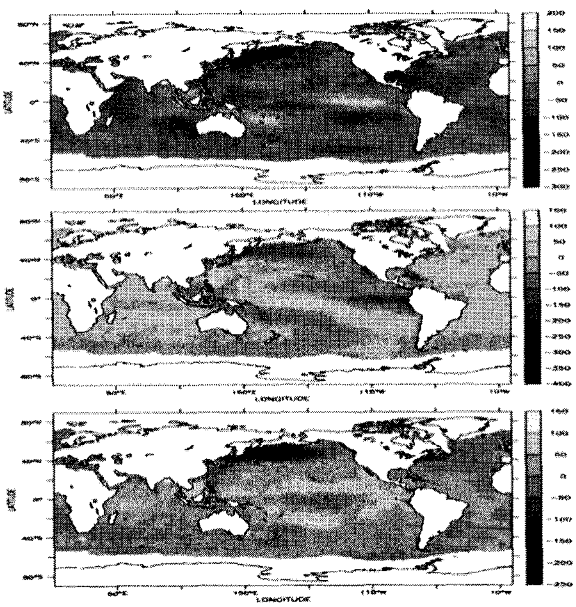

Figure 4. Spatial distribution of eigenfunctions

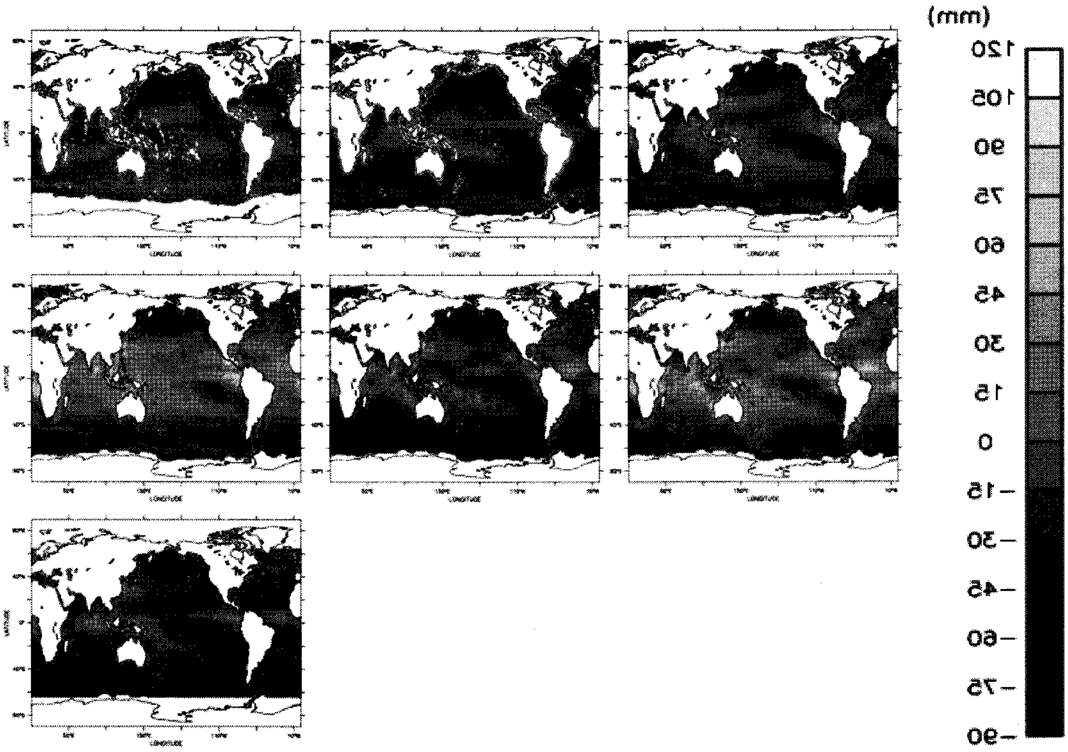

Figure 5. Average differences (a. GSSTF2, b. HOAPS3, c.ERA40, d. JRA25, e. NRA1, f. NRA2, and g. OA Flux - J-OFURO2 evaporation).

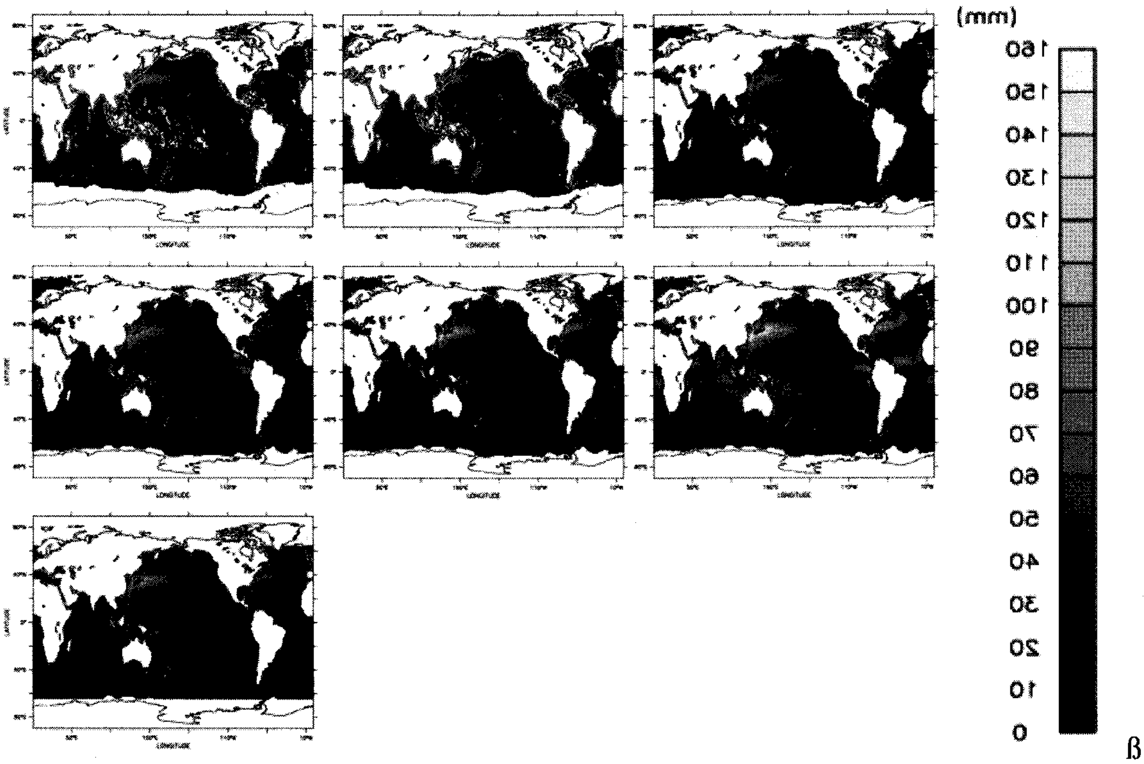

Figure 6. RMS differences (a. GSSTF2, b. HOAPS3, c.ERA40, d. JRA25, e. NRA1, f. NRA2, and g. OA Flux - J-OFURO2 evaporation